

Single- and two-nucleon antikaon absorption in nuclear matter with chiral meson-baryon interactions

Jaroslava Hrtáková

Nuclear Physics Institute, Řež

Àngels Ramos

University of Barcelona, Barcelona

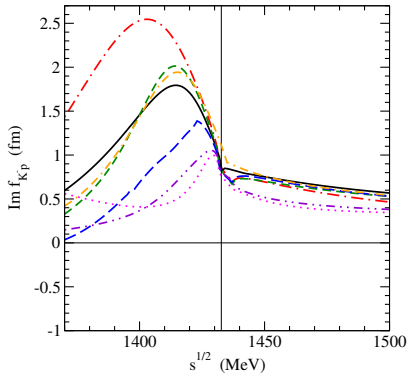
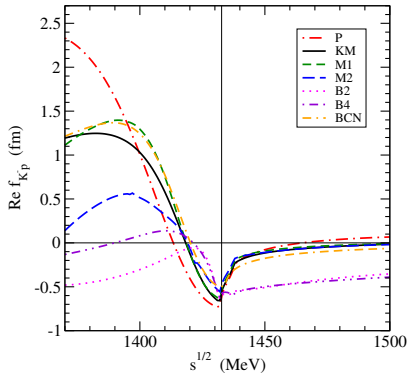


STRANEX workshop, ECT* Trento, Italy, 21 - 25 October, 2019

Introduction

- K^- multi-nucleon absorption fraction in the surface region of atomic nuclei represents about 20%
NC 53 (1968) 313 (Berkeley), NPB 35 (1971) 332 (BNL), NC 39A (1977) 538 (CERN)
- It was described mainly by phenomenological optical potential so far
E. Friedman, A. Gal, NPA 959 (2017) 66
- Previous model for $K^- NN$ absorption in nuclear matter using free-space chiral amplitudes by *T. Sekihara et al., PRC 86 (2012) 065205*
- New experimental data on $K^- NN$ absorption (AMADEUS@DAΦNE)
K. Piscicchia et al., PLB 782 (2018) 339
R. Del Grande et al., EPJ C79 (2019) 190
- Solid microscopic model for $K^- NN$ absorption needed

Free-space $K^- p$ amplitudes in various chiral models



Prague (P)

Kyoto-Munich (KM)

Murcia (M1 and M2)

Bonn (B2 and B4)

Barcelona (BCN)

A. Cieply, J. Smejkal, *Nucl. Phys. A* 881 (2012) 115

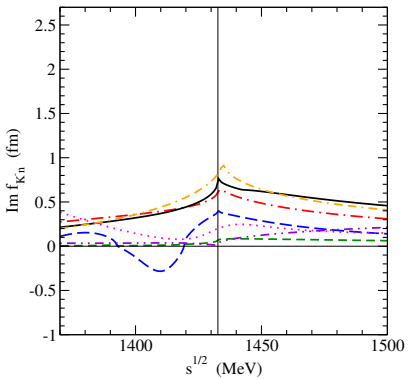
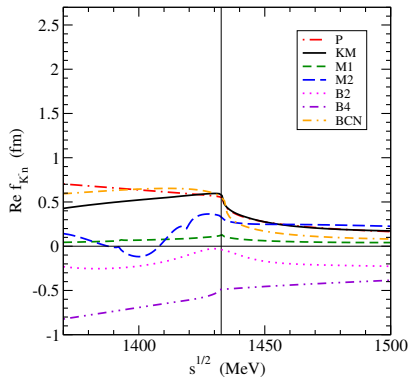
Y. Ikeda, T. Hyodo, W. Weise, *Nucl. Phys. A* 881 (2012) 98

Z. H. Guo, J. A. Oller, *Phys. Rev. C* 87 (2013) 035202

M. Mai, U.-G. Meißner, *Nucl. Phys. A* 900 (2013) 51

A. Feijoo, V. Magas, A. Ramos, *Phys. Rev. C* 99 (2019) 035211

Free-space K^-n amplitudes



Kaonic atoms

- Info about K^-N interaction below threshold provided by kaonic atoms
65 data points (energy shifts, widths, yields=upper level widths)
from CERN, Argonne, RAL, BNL
- Chirally motivated models fail to describe kaonic atom data
E. Friedman, A. Gal, NPA 959 (2017) 66

M multinucleon processes

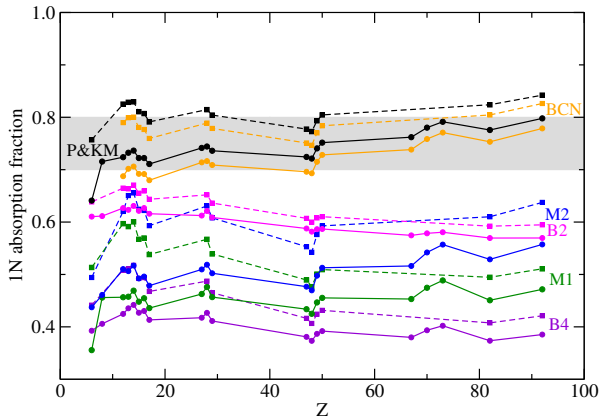
- Chiral models include only $K^- N \rightarrow \pi Y$ ($Y = \Lambda, \Sigma$) decay channel
- K^- interactions with two and more nucleons should be included,
(e.g., $K^- + N + N \rightarrow Y + N$) - recent analysis of kaonic atom data
E. Friedman, A. Gal, NPA 959 (2017) 66

$$2\text{Re}(\omega_{K^-})V_{K^-}^{(2)} = -4\pi B\left(\frac{\rho}{\rho_0}\right)^\alpha \rho ,$$

where B is a **complex** amplitude, ρ is nuclear density distribution, ρ_0 is saturation density and α is positive

- Amplitude B fitted for each chiral model separately

Single- vs. multi-nucleon processes



- Fraction of *single-nucleon* absorption 0.75 ± 0.05 (average value) applied as an **additional constraint**.

→ Only P, KM and BCN models found acceptable in kaonic atom analysis
E. Friedman, A. Gal, NPA 959 (2017) 66

Microscopic model for K^-NN absorption in nuclear matter

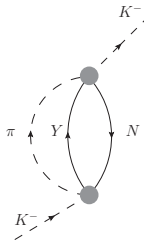
We have developed microscopic model for K^- two-nucleon absorption in symmetric nuclear matter

J. Hrtáňková, Á. Ramos, arXiv:1910.01336 [nucl-th], submitted to PRC

- based on a meson-exchange approach
H. Nagahiro et al., PLB 709 (2012) 87.
- employing P and BCN chiral K^-N amplitudes
- considering Pauli correlations in the medium for K^-N amplitudes
- real part of the K^-NN optical potential evaluated as well
- K^-N optical potential derived within the same approach

$K^- N$ absorption in nuclear matter

$$K^- N \rightarrow \pi Y \quad (Y = \Lambda, \Sigma)$$



- $K^- N$ self-energy

$$\Pi_{K^- N \rightarrow \pi Y}(\vec{p}, p_0) = i |t_{K^- N \rightarrow \pi Y}|^2 \int \frac{d^4 q}{(2\pi)^4} U_{YN}(p - q) \frac{1}{q^2 - m_\pi^2 + i\eta}$$

t - two-body t-matrix; U - Lindhard function

p - kaon 4-momentum; q - meson 4-momentum

$K^- NN$ absorption in nuclear matter

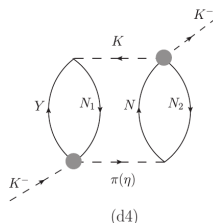
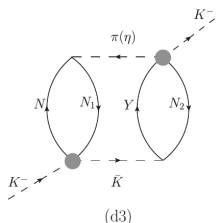
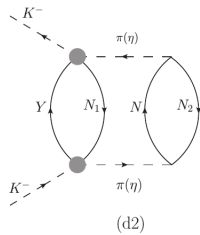
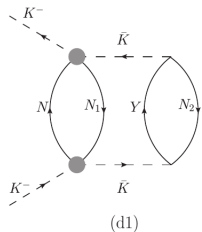


Fig.1: Two-fermion-loop (2FL) Feynman diagrams for non-mesonic K^- absorption on two nucleons N_1 , N_2 in nuclear matter. The shaded circles denote the K^-N t-matrices derived from a chiral model.

$K^- NN$ absorption in nuclear matter

- $K^- NN$ self-energy from a direct 2FL diagram

$$\begin{aligned}\Pi_{K^- NN}^{2\text{FL}}(\vec{p}, p_0) = & -it_{B_1 x} t_{B_1 x}^* V_{B_2 N_2 x} V_{B_2 N_2 x} \int \frac{d^4 q}{(2\pi)^4} U_{B_1 N_1}(p - q) U_{B_2 N_2}(q) \\ & \times (-\vec{q}^2) \frac{1}{q^2 - m_x^2 + i\eta} \frac{1}{q^2 - m_x^2 + i\eta} ,\end{aligned}$$

$x = K^-, \bar{K}^0, \pi, \eta$; t - two-body t-matrices; $B_1, B_2 = N, Y$

V - meson-baryon-baryon couplings; U - Lindhard function

p - kaon 4-momentum, q - meson 4-momentum

- Contributions from diagrams (d3) and (d4) are zero due to null trace over spins

$K^- NN$ absorption in nuclear matter

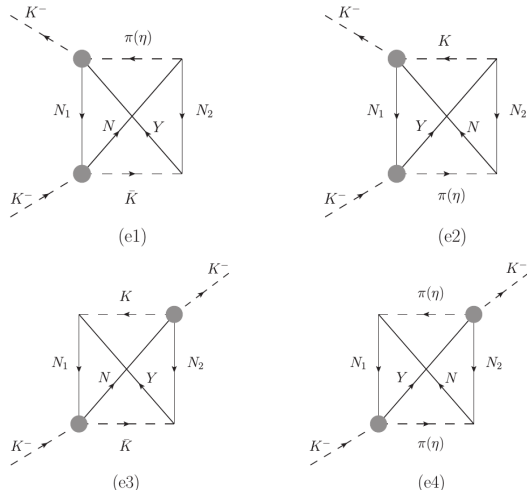


Fig.2: One-fermion-loop (1FL) Feynman diagrams for non-mesonic K^- absorption on two nucleons N_1 , N_2 in nuclear matter. The shaded circles denote the K^-N t-matrices derived from a chiral model.

$K^- NN$ absorption in nuclear matter

- $K^- NN$ self-energy from an exchange 1FL diagram

$$\begin{aligned}\Pi_{K^- NN}^{1\text{FLA}}(\vec{p}, p_0) &= -i t_{B_1 x_1} t_{B_2 x_2}^* V_{B_2 N_2 x_1} V_{B_1 N_2 x_2} \int \frac{d^4 q}{(2\pi)^4} (+2\vec{q}^2) \\ &\quad \times \int \frac{d^4 j}{(2\pi)^4} G_{N_1}(j) G_{B_1}(j + p - q) \int \frac{d^4 k}{(2\pi)^4} G_{N_2}(k) G_{B_2}(q + k) \\ &\quad \times \frac{1}{q^2 - m_{x_1}^2 + i\eta} \frac{1}{q'^2 - m_{x_2}^2 + i\eta} = \\ &= i t_{B_1 x_1} t_{B_2 x_2}^* V_{B_2 N_2 x_1} V_{B_1 N_2 x_2} \frac{1}{2} \int \frac{d^4 q}{(2\pi)^4} U_{B_1 N_1}(p - q) U_{B_2 N_2}(q) \\ &\quad \times \vec{q}^2 \frac{1}{q^2 - m_{x_1}^2 + i\eta} \frac{1}{q'^2 - m_{x_2}^2 + i\eta}\end{aligned}$$

G - baryon propagator in the medium; j, k - nucleon 4-momenta

$K^- NN$ absorption in nuclear matter

- K^- self-energy related to optical potential $V_{K^-} = \frac{\Pi_{K^-}}{2E_{K^-}}$
- $V_{K^-N} = \sum_{channels} V_{K^-N \rightarrow \pi Y}$
- $V_{K^-NN} = \sum_{channels} V_{K^-NN}^{2FL} + V_{K^-NN}^{1FL}$
 - contributions from 37 2FL and 28+33 1FL diagrams

Table 1: All considered channels for mesonic and non-mesonic K^- absorption in matter.

$K^- N$	$\rightarrow \pi Y$	$K^- N_1 N_2$	$\rightarrow Y N$
$K^- p$	$\rightarrow \pi^0 \Lambda$	$K^- pp$	$\rightarrow \Lambda p$
	$\rightarrow \pi^0 \Sigma^0$		$\rightarrow \Sigma^0 p$
	$\rightarrow \pi^+ \Sigma^-$		$\rightarrow \Sigma^+ n$
	$\rightarrow \pi^- \Sigma^+$	$K^- pn(np)$	$\rightarrow \Lambda n$
$K^- n$	$\rightarrow \pi^- \Lambda$		$\rightarrow \Sigma^0 n$
	$\rightarrow \pi^- \Sigma^0$		$\rightarrow \Sigma^- p$
	$\rightarrow \pi^0 \Sigma^-$	$K^- nn$	$\rightarrow \Sigma^- n$

K^-N free-space vs. Pauli blocked scattering amplitudes

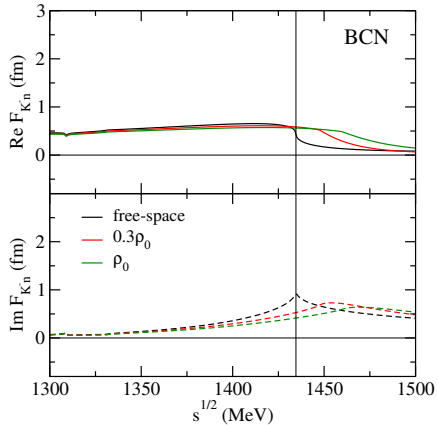
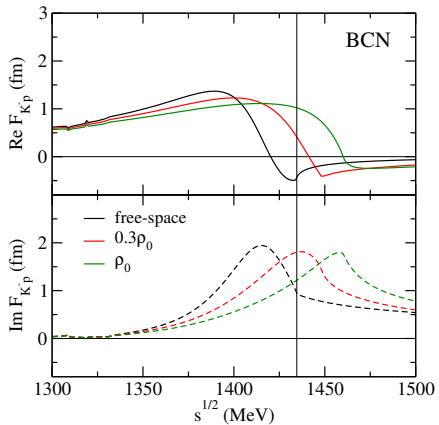
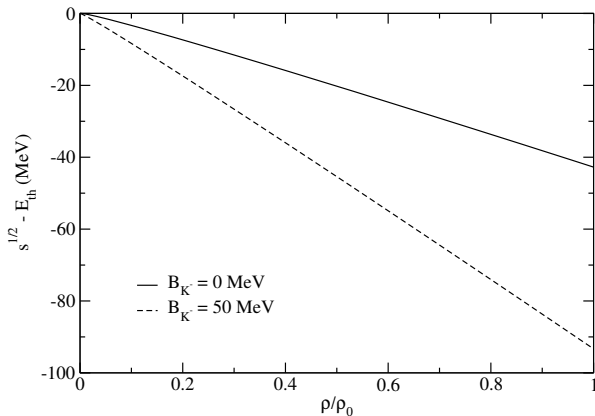


Fig.3: Comparison of K^-p and K^-n free-space (black) and Pauli blocked amplitudes at two different nuclear matter densities: $0.3\rho_0$ (red) and ρ_0 (green), calculated in the BCN model.

Energies probed below K^-N threshold

- Energy shift $\delta\sqrt{s} = \sqrt{s} - E_{\text{th}}$ where $\sqrt{s} = \sqrt{(E_{K^-} + E_F)^2 - \frac{3}{5}k_F^2}$,

$E_F = \sqrt{m_N^2 + \frac{3}{5}k_F^2} + V_N \frac{\rho}{\rho_0}$ with $V_N = -50$ MeV, $E_{K^-} = m_{K^-} - B_{K^-} \frac{\rho}{\rho_0}$,
 k_F - Fermi momentum, $\rho_0 = 0.169$ fm $^{-3}$, $E_{\text{th}} = m_N + m_{K^-}$



K^- potential in nuclear matter - medium effects

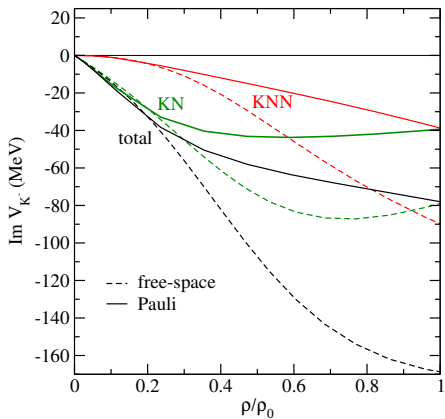
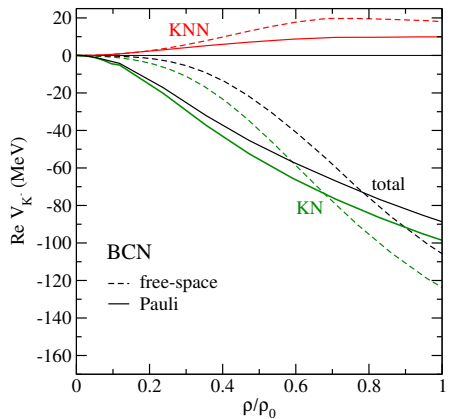


Fig.4: The real (left) and imaginary (right) parts of the K^-N , K^-NN , and total optical potentials as a function of relative density, calculated using the free-space (dashed) and Pauli blocked (solid) BCN amplitudes for $B_{K^-} = 0$ MeV.

K^-N and K^-NN absorption fractions

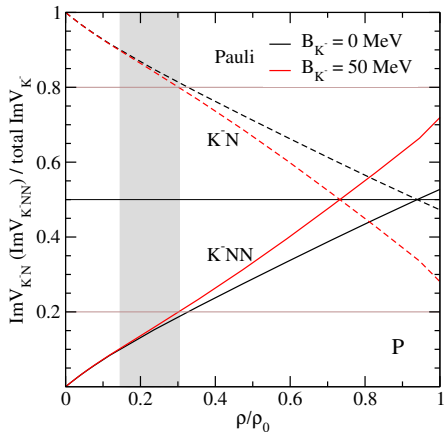
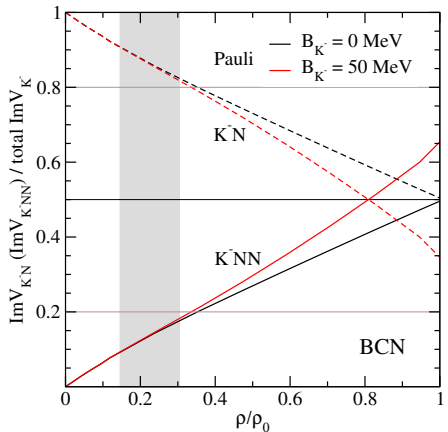


Fig.5: Ratio of K^- single-nucleon (K^-N) and two-nucleon (K^-NN) absorptive potentials to the total K^- absorptive potential as a function of relative density, calculated using the Pauli blocked amplitudes and for $B_{K^-} = 0$ and 50 MeV . The gray band denotes the region of densities probed in experiments with low-energy K^- .

AMADEUS data

- New measured ratio *R. Del Grande et al., EPJ C79 (2019) 190*

$$R = \frac{\text{BR}(K^- pp \rightarrow \Lambda p)}{\text{BR}(K^- pp \rightarrow \Sigma^0 p)} = 0.7 \pm 0.2(\text{stat.})^{+0.2}_{-0.3}(\text{syst.})$$

- Assumption that dominant contribution for $K^- pp \rightarrow \Lambda p$ and $K^- pp \rightarrow \Sigma^0 p$ channels comes from π^0 exchange leads to relation

$$\frac{\text{BR}(K^- pp \rightarrow \Lambda p)}{\text{BR}(K^- pp \rightarrow \Sigma^0 p)} = \frac{\text{BR}(K^- p \rightarrow \pi^0 \Lambda)}{\text{BR}(K^- p \rightarrow \pi^0 \Sigma^0)}$$

- However, the dominant contribution for $K^- pp \rightarrow \Lambda p$ channel comes from K^- exchange!

T. Sekihara, D. Jido, Y. Kanada-En'yo, PRC 79 (2009) 062201(R)

J. Hrtáčková, Á. Ramos, arXiv:1910.01336 [nucl-th], submitted to PRC

Ratio R for 2N absorption

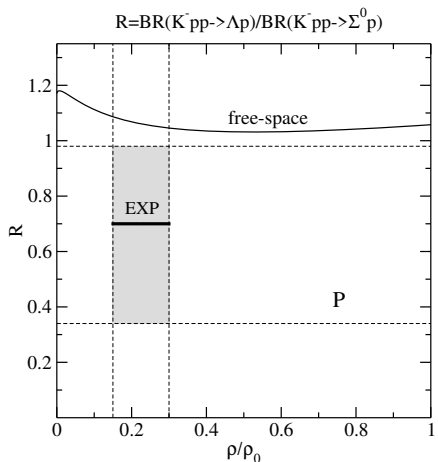
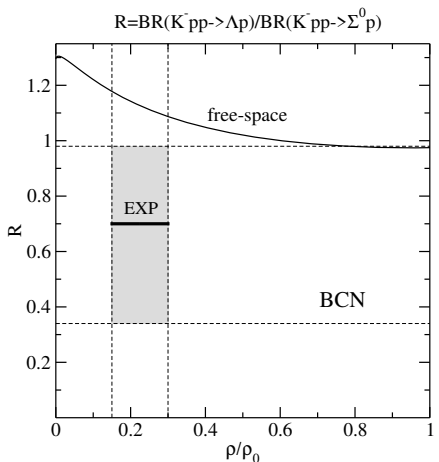


Fig.6: The ratio R as a function of relative density, calculated using the free-space amplitudes for $B_{K^-} = 0$ MeV. The dashed vertical lines denote the region of densities probed in experiments with low-energy K^- including the experimental value of the ratio with corresponding error bar.

Ratio R for $2N$ absorption

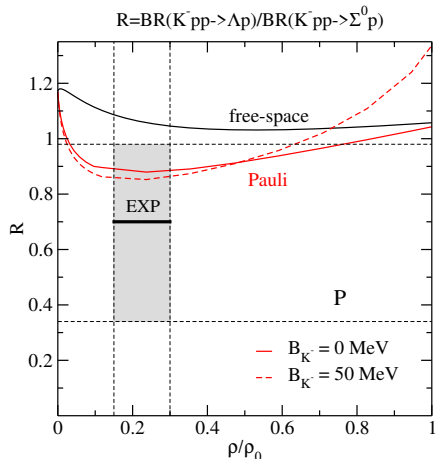
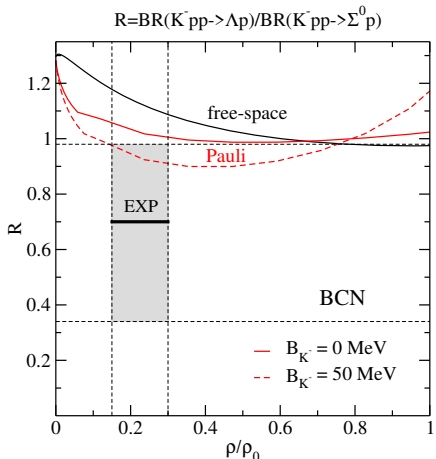


Fig.7: The ratio R as a function of relative density, calculated using the free-space and Pauli blocked amplitudes for $B_{K^-} = 0$ MeV and $B_{K^-} = 50$ MeV. The dashed vertical lines denote the region of densities probed in experiments with low-energy K^- including the experimental value of the ratio with corresponding error bar.

Ratio R^* for 1N absorption

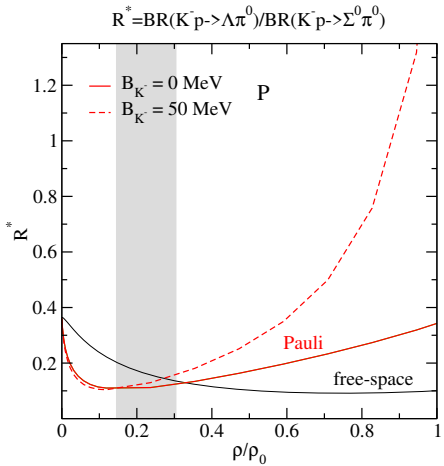
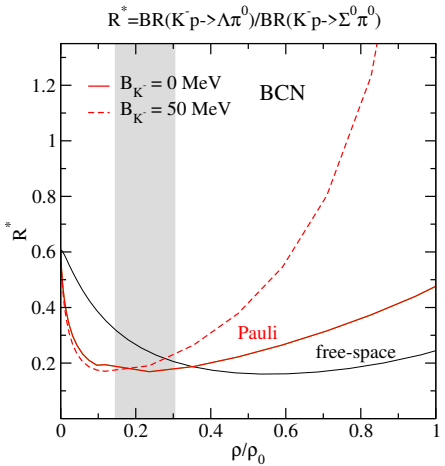


Fig.8: The ratio R^* as a function of relative density, calculated using the free-space and Pauli blocked amplitudes for $B_{K^-} = 0 \text{ MeV}$ and $B_{K^-} = 50 \text{ MeV}$. The gray band denotes the region of densities probed in experiments with low-energy K^- .

Comparison with experimental data

Table 2: Primary-interaction ratios (in %) for mesonic absorption of K^- in nuclear matter, calculated with free-space and Pauli blocked BCN amplitudes for $B_{K^-} = 0$ MeV. The experimental data corrected for primary^a interaction are shown for comparison.

BCN	0.3 ρ_0		0.5 ρ_0		Exp. [1]	
	f.s.	Pauli	f.s.	Pauli	${}^4\text{He}$	${}^{12}\text{C}$
$\Sigma^+ \pi^- / K^-$	19.0	28.0	21.4	27.6	31.2 ± 5.0	29.4 ± 1.0
$\Sigma^- \pi^0 / K^-$	6.0	5.5	4.2	5.3	4.9 ± 1.3	2.6 ± 0.6
$\Sigma^- \pi^+ / K^-$	21.3	14.4	15.8	9.3	9.1 ± 1.6	13.1 ± 0.4
$\Sigma^0 \pi^- / K^-$	6.0	5.6	4.2	5.4	4.9 ± 1.3	2.6 ± 0.6
$\Sigma^0 \pi^0 / K^-$	17.6	18.7	16.9	16.0	17.7 ± 2.9	20.0 ± 0.7
$\Lambda \pi^0 / K^-$	3.7	3.4	2.8	3.5	5.2 ± 1.6	3.4 ± 0.2
$\Lambda \pi^- / K^-$	7.4	6.8	5.6	7.2	10.5 ± 3.0	6.8 ± 0.3
total 1N ratio	81.0	82.4	70.9	74.3	83.5 ± 7.1	77.9 ± 1.6

^a Corrected for secondary interactions of the primary particles created in the absorbing nucleus.

[1] C. Vander Velde-Wilquet et al., *Nuovo Cimento* 39 A (1977) 538

Comparison with experimental data

Table 3: Primary-interaction total ratios (in %) for non-mesonic and total (1N+2N) K^- absorption in matter and corresponding ratios corrected for Σ - Λ conversion with different conversion rates, a) - 60% for $\Sigma^+ \text{-} \Lambda$, 22.5% for $\Sigma^- \text{-} \Lambda$, 72% for $\Sigma^0 \text{-} \Lambda$, b) - 50% for all Σ 's, calculated with Pauli blocked BCN amplitudes for $B_{K^-} = 0$ MeV.

BCN	$0.3\rho_0$	$0.3\rho_0 + \Sigma\text{-}\Lambda$ conv.		Exp. [2]
non-mesonic ratio		a)	b)	${}^4\text{He}$
$(\Lambda N + \Sigma^0 N)/K^-$	8.3	12.0	12.9	11.7 ± 2.4
$\Sigma^- N/K^-$	4.9	3.8	2.5	3.6 ± 0.9
$\Sigma^+ N/K^-$	4.3	1.7	2.2	1.0 ± 0.4
$\Sigma^0 N/K^-$	4.2	1.2	2.1	2.3 ± 1.0
total 2N ratio	17.6	17.6		16.4 ± 2.6
total ratio				
Σ^+ / K^-	32.3	12.9	16.2	17.0 ± 2.7
Σ^- / K^-	24.8	19.2	12.4	13.8 ± 1.8
Σ^0 / K^-	28.5	8.0	14.3	10.8 ± 5.0
Λ / K^-	14.3	59.8	57.2	58.4 ± 5.7
Σ^+ / Σ^-	1.3	0.7	1.3	1.2 ± 0.2

Conclusions

- Interaction of K^- with two and more nucleons important for realistic description of K^- -nucleus interaction
- We have developed a microscopic model for K^-NN absorption in nuclear matter using scattering amplitudes derived from P and BCN chiral meson-baryon interaction models

J. Hrtánková, Á. Ramos, arXiv:1910.01336 [nucl-th], submitted to PRC

- Pauli blocked amplitudes included → medium effects non-negligible
- Calculated ratios in a good agreement with experimental data!
- Further application of the model in the calculations of kaonic atoms and K^- -nuclear quasibound states

Backup

Backup slides

Free-space vs. Pauli blocked amplitudes

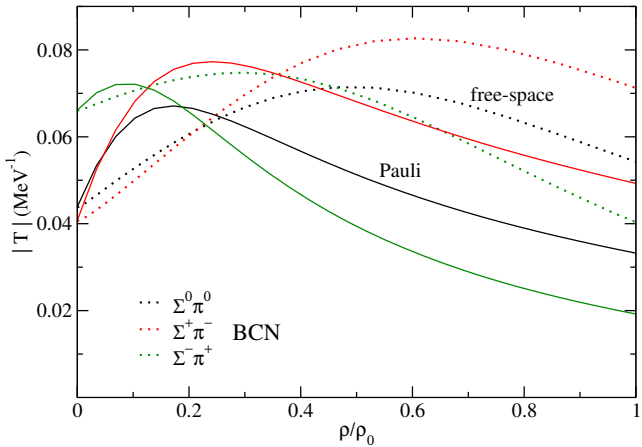


Fig.9: Absolute values of $\Sigma^0 \pi^0$ (black), $\Sigma^+ \pi^-$ (red), and $\Sigma^- \pi^+$ (green) free-space (dotted) and Pauli blocked (solid) BCN model t-matrices as functions of relative density ρ/ρ_0 , printed for energy shift corresponding to $B_{K^-} = 0$ MeV.

K^- potential in nuclear matter

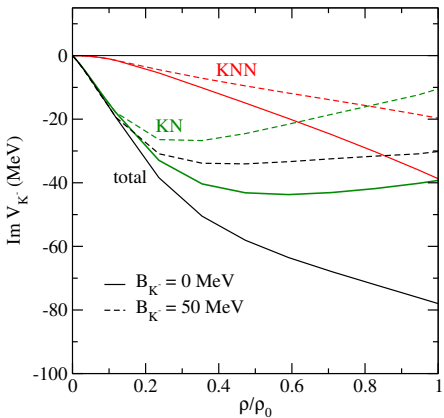
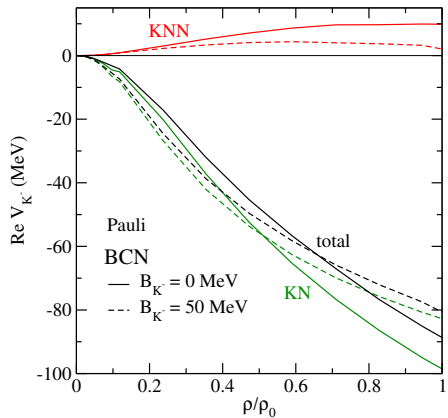


Fig.10: Real (left) and imaginary (right) parts of the $K^- N$, $K^- NN$, and total optical potential as a function of relative density, calculated using the Pauli blocked BCN amplitudes for $B_{K^-} = 0$ and 50 MeV.